16th World Conference on Earthquake Engineering, 16WCEE 2017

Santiago Chile, January 9th to 13th 2017

Paper N°_3832

Registration Code: S-J1463692100

EFFECT OF OUT-OF-PLANE LOADING ON THE IN-PLANE RESPONSE OF SC WALL PIERS

B. Terranova (1), S. Epackachi (2), A. S. Whittaker (3)

(1) *PhD Candidate, Dept. of Civil, Structural and Environmental Engineering, University at Buffalo, Buffalo, NY 14260. Email: brt2@buffalo.edu*

(2) *Teaching Assistant Professor, Dept. of Civil, Structural and Environmental Engineering, University at Buffalo, Buffalo, NY 14260. Email: siamakep@buffalo.edu*

(3) *Professor; Director, MCEER; Dept. of Civil, Structural and Environmental Engineering, University at Buffalo, Buffalo, NY 14260. Email: awhittak@buffalo.edu*

Abstract

Steel-plate concrete (SC) composite shear walls are typically composed of steel faceplates, infill concrete, shear studs bonding the faceplate to the infill, and tie rods linking the faceplates. To date, most studies of these shear walls have focused on in-plane (IP) response and the effects of co-existing out-of-plane (OOP) loading have not been considered.

Numerical studies are conducted to investigate the effect of OOP loading (magnitude and location) on the IP response of SC wall piers with different aspect ratios, reinforcement ratios, and axial loads, using the general-purpose finite element code LS-DYNA. The baseline LS-DYNA model was validated for IP behavior using data from the tests of large-scale rectangular SC wall piers and for OOP behavior using data from tests of singly reinforced concrete specimens without shear reinforcement. The results of the parametric studies show that OOP loading has a significant effect on the IP capacity of SC wall piers; the effects become more significant as the shear span-to-depth ratio and magnitude of the OOP load are increased. As the magnitude of the axial compressive load applied to SC wall and/or the faceplate reinforcement ratio increase, the percentage reduction in IP lateral capacity is decreased.

Keywords: Composite shear wall; out-of-plane loading; cyclic loading; LS-DYNA; numerical model.

1. Introduction

Steel-plate concrete (SC) composite walls consisting of steel faceplates, infill concrete, and connectors used to anchor the steel faceplates together to the infill concrete may be a viable construction alternative to reinforced concrete (RC) and steel plate shear walls. Double skin SC wall shells can be fabricated offsite, assembled and filled on-site with concrete to create a monolithic wall. The use of steel faceplates by-and-large eliminates the need for formwork, and the plates serve as primary reinforcement. The challenges associated with SC walls include joining the shells in the field, field inspection of the concrete behind the faceplates, and the interaction of co-existing in-plane (IP) and out-of-plane (OOP) loadings that has not yet been adequately characterized.

The IP behavior of SC walls has been studied extensively, numerically and experimentally. However, there is limited information on the OOP behavior of SC walls. Yang et al. [1] executed three full-scale experiments investigating the OOP cyclic behavior of SC walls. The parameters considered in that study were shear span-to-depth ratio and steel faceplate thickness, where the shear span-to-depth ratio for OOP loading is defined as the vertical distance between the line of OOP loading and the base of the wall divided by the wall thickness. Sener et al. [2, 3] conducted large scale, one-way bending tests on SC beams specimens, representative of strips in the longitudinal and transverse directions of SC walls, to investigate OOP shear and flexural behaviors. They compiled a database of test results and used it to evaluate design codes, and concluded that the ACI 349M-06 [4] equations for RC beams and slabs could be used to predict OOP shear strength (for shear span-to-depth ratios larger than 3) and the OOP flexural capacity of SC walls (for any shear span-to-depth ratios). Bhardwaj et al. [5] investigated the effects of OOP forces on the IP capacity of SC walls using numerical tools developed in LS-DYNA by Kurt et al. [6] for IP behavior. The results of a limited number of numerical simulations indicated that the shear span-to-depth ratio and the magnitude of the OOP load significantly affect the IP capacity of SC wall piers. Other parameters including axial load, reinforcement ratio, and aspect ratio were not investigated.

The research published to date on the behavior of SC walls under IP and OOP loadings is limited. Herein, a validated LS-DYNA model is used to conduct a parametric study that investigates the effect of OOP loading on the IP response of SC walls. The key design variables considered in this study are aspect ratio, reinforcement ratio, axial load, shear span-to-depth ratio for OOP loading, and magnitude of the OOP load.

2. Validation of numerical model for in-plane and out-of-plane loadings

2.1 In-plane response

The general-purpose finite element code LS-DYNA [7, 8] was used to develop a reliable finite element model for the nonlinear cyclic analysis of flexure-critical SC walls. The LS-DYNA model was validated using the results of cyclic tests of the IP behavior of four large-scale rectangular SC walls (SC1 through SC4) tested at the University at Buffalo [9, 10, 11]. The aspect ratio of all four walls was 1.0. The design parameters considered in the experiments were wall thickness (9 in. and 12 in.), reinforcement ratio (3.1% and 4.2%), and faceplate slenderness ratio (21, 24, and 32). A photograph of specimen SC1 is presented in Fig. 1a. Fig. 1b presents the LS-DYNA model of SC1. The infill concrete and the steel faceplates were modeled using the smeared crack Winfrith model, MAT085, and the plastic-damage, MAT081, available in LS-DYNA, respectively. Beam elements were used to represent the studs and tie rods. Eight-node solid elements were used to model the infill concrete and the base plates, and four-node shell elements were used for the steel faceplates. A penalty-based approach, CONTACT-AUTOMATIC-SURFACE-TO-SURFACE formulation, was used to model the friction between the infill concrete and the steel faceplates. A tie constraint was used to attach the studs and tie rods to the steel faceplates and the baseplate. The connectors were tied to the infill concrete elements using LAGRANGE-IN-SOLID constraint.

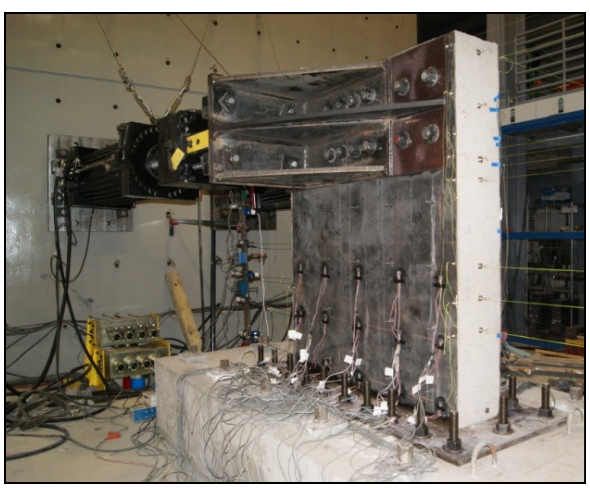

(a) test specimen

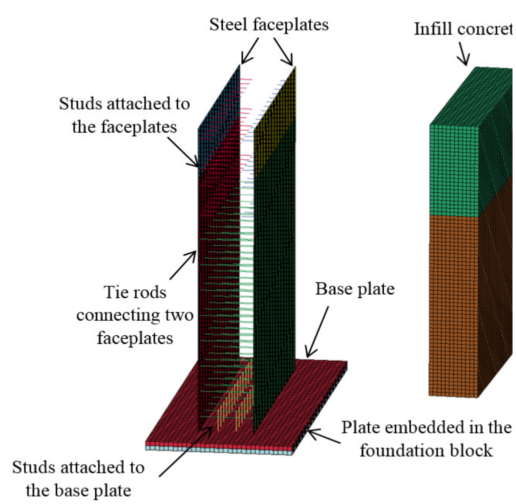

(b) LS-DYNA model

Fig. 1 – Photograph and LS-DYNA model of SC1 [9]

The LS-DYNA model was validated through comparisons of predictions and measurements of the cyclic force-displacement relationships, equivalent damping ratios, shearing forces in the steel faceplates, the deformed shapes of the steel faceplates, and the Von-Mises stress distributions in the steel faceplates. The predicted and measured cyclic force-displacement relationships of SC2 and SC4 are presented in Fig. 2. As seen in Fig. 2, the predicted peak strength, initial stiffness, pinching, and rate of reloading/unloading stiffness match the experimental results. The validation study is described in detail in Epackachi et al. [11]. Epackachi et al. then used this validated LS-DYNA model to derive simplified analytical models suitable for preliminary analysis and design of SC walls [12], and to conduct a parametric study that investigated the effects of key design variables including wall aspect ratio, reinforcement and slenderness ratios, axial load, and steel and concrete strengths on the IP response of SC walls [13].

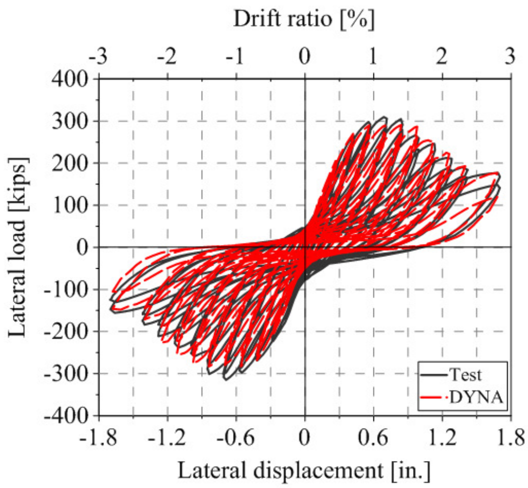

(a) SC2

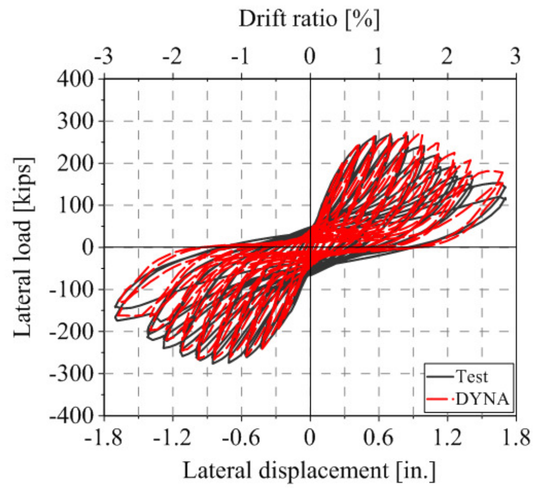

(b) SC4

Fig. 2 – Predicted and measured lateral load - displacement relationships of SC walls

2.2 Out-of-plane response

Data from tests of singly reinforced RC specimens without shear reinforcement performed by Bresler et al. [14] and Mphonde et al. [15] were used to validate the Winfrith concrete model for predictions of OOP shear behavior in SC walls. In the absence of shear reinforcement, concrete plays the primary role in resisting shearing OOP forces in both RC and SC walls. Validation of a concrete model using data from tests of RC specimens without shear reinforcement serves to validate it for OOP analysis of SC specimens. Information on the dimensions of the RC test specimens and the material properties used in LS-DYNA simulations are summarized in Table 1, where w, h and l are the width, height, and length of the beam specimens, respectively, $f_c^{'}$ is the compressive strength of the concrete, $f_t^{'}$ is the tensile strength of the concrete (taken as $0.1f_c^{'}$ unless specified in the experiment), ρ_w is the longitudinal reinforcement ratio, E is the elastic modulus defined as $E = 57000\sqrt{f_c^{'}}$, G is the fracture energy, and w^* is the crack width defined as $w^* = 2G / f_t^{'}$. The fracture energy, which is defined as the area under the tensile stress-displacement curve [16], was estimated using Equation 2.1-7 or Table 2.1.4 of the CEB-FIP Model Code [17]. Bresler et al. [14] performed Test 1. Mphonde et al. [15] performed Tests 2 through 6. In these experiments, the shear span-to-depth ratio, a / d, was varied from 1.5 to 4 and the concrete compressive strength was varied from 3200 to 10634 psi.

Table 1 - Specimen dimensions and material properties input to the LS-DYNA model

Test	Beam dimensions $w \times h \times l$ (in × in × in)	a/d	$f_c^{'}$ (psi)	$f_t^{'}$ (psi)	ρ_w (%)	E ($\times 10^6$ psi)	G (lb-in/in^2)	w^* (in)
1	12 × 21.75 × 144	4	3270	575	1.8	3.26	0.371	0.0013
2	6 × 13.25 × 96	3.6	3273	327	3.36	3.26	0.371	0.0023
3	6 × 13.25 × 96	2.5	3246	325	3.36	3.25	0.371	0.0023
4	6 × 13.25 × 96	1.5	3637	364	3.36	3.44	0.399	0.0022
5	6 × 13.25 × 96	1.5	6593	364	3.36	4.63	0.548	0.0017
6	6 × 13.25 × 96	1.5	10634	364	3.36	5.88	0.714	0.0014

Fig. 3 presents the test setup for the Bresler experiment. The LS-DYNA model used for the analysis of the Bresler's specimen is presented in Fig. 4. Beam elements were used to model the longitudinal reinforcement (4 #9 bars with a 1-inch cover, corresponding to a reinforcement ratio of 1.8%). The 1 × 1 × 1 in. eight-node solid elements were used to model the concrete beam. The rebar was embedded into the concrete using node sharing. The constant stress formulation (ELFORM=1 in LS-DYNA) and cross section integrated beam element (Hughes-Liu beam in LS-DYNA) were used for the solid and beam elements, respectively. The Winfrith concrete model, MAT085, was used to model the concrete. The d3crack database was activated to visualize the crack pattern during loading. The PIECEWISE_LINEAR_PLASTICITY material model, MAT024, was used to model the Grade 60 reinforcement. The pin and roller boundary conditions were applied by constraining the displacements of three rows of the nodes, corresponding to three inches at each support, in the Y and Z directions.

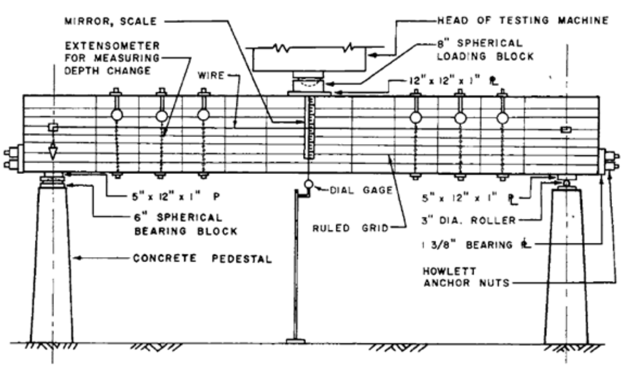

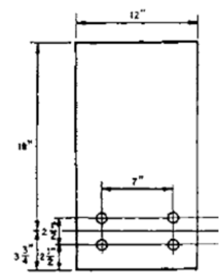

(a) test setup (b) cross-section of the beam specimen

Fig. 3 – Beam tested by Bresler et al. [14]

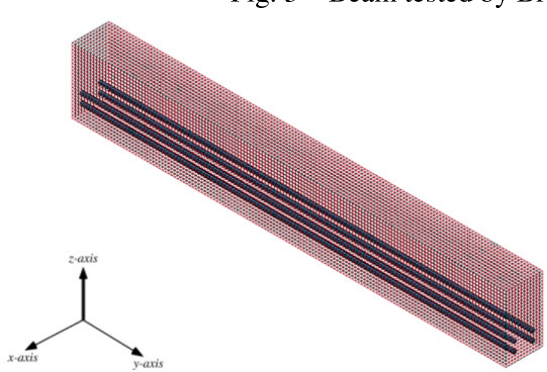

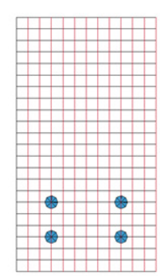

(a) view of model (b) cross-section

Fig. 4 – LS-DYNA model for the analysis of the Bresler specimen

Fig. 5a and 5b present the predicted and measured crack patterns at failure, respectively. The LS-DYNA model reasonably predicted the observed damage. Cracking at the support caused by slippage of the longitudinal reinforcement was not captured in the simulation because the longitudinal reinforcement was numerically tied to the concrete elements. Fig. 5c presents the predicted and measured force-displacement relationships at the center of the beam. The predicted OOP force-displacement relationship agrees well with the experimental result.

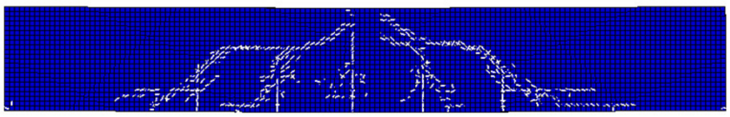

(a) predicted damage

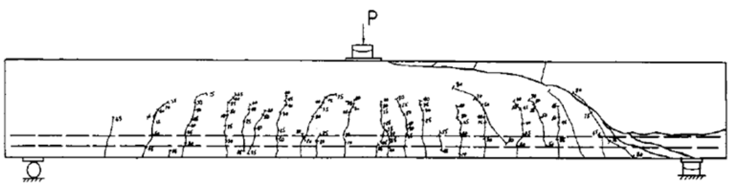

(b) measured damage

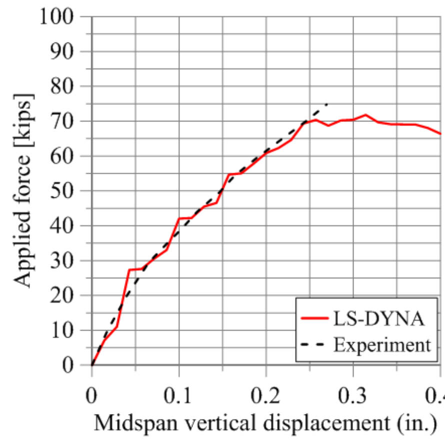

(c) predicted and measured force-displacement relationships

Fig. 5 – Predicted and measured responses of the Bresler beam

Fig. 6 presents the beam specimen tested by Mphonde et al. [15]. The longitudinal reinforcement consists of three #8 bars with 1 in. of cover, which corresponds to a reinforcement ratio of 3.36%. The values of the input parameters for the LS-DYNA simulations are presented in Table 1: Tests 2 through 6. The material models and element types used for the Bresler beam were adopted for analysis of Tests 2 through 6. The constraints were moved to accommodate the different spans. Loading was simulated by imposing displacements at the nodes of the concrete elements located in a vertical plane at the mid-span of the beam. Table 2 enables a comparison of the LS-DYNA simulations and the test results. The simulations accurately recover the maximum shear stress calculated from the experiments, which cover a wide range of a/d.

These comparisons of predicted and measured responses indicate that the Winfrith concrete model can be used to simulate the OOP behavior of RC and SC walls under monotonic loading to failure.

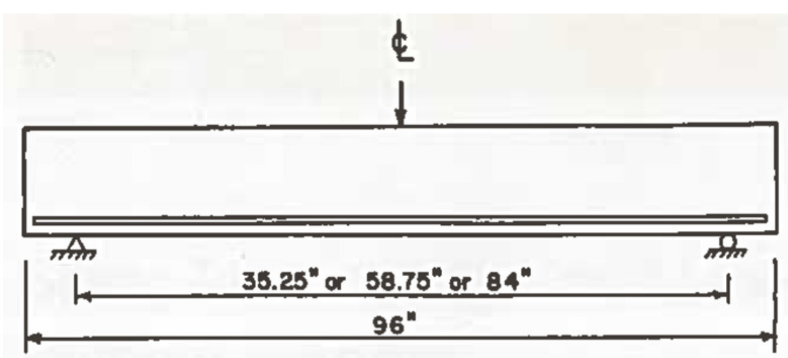

(a) beam specimen

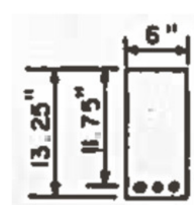

(b) cross-section of the beam specimen

Fig. 6 – Experimental setup for Mphonde et al. [15]

Table 2 – Results of RC beam simulations at peak load

Test	a / d	Shear stress (psi)		Difference (%)
		Experiment	LS-DYNA	
2	3.6	206	198	4
3	2.5	248	302	18
4	1.5	370	379	2
5	1.5	993	974	2
6	1.5	1379	1371	-

3. The effects of OOP loading on the IP response of SC wall piers

Bhardwaj et al. [5] introduce a research project funded by the Canadian Nuclear Safety Commission (CNSC) on the effects of OOP loading on the IP capacity of SC walls [5]. Three large-scale rectangular SC wall specimens (CNSC1 through CNSC3) were proposed for testing under combined IP and OOP loadings. An LS-DYNA model of CNSC1 forms the basis of the studies described below, which investigate the effect of aspect ratio, reinforcement ratio, axial load, shear span-to-depth ratio for OOP loading, and magnitude of the OOP loading, on the IP response of SC walls. The LS-DYNA model of CNSC1, shown in Fig. 7, is composed of infill concrete, baseplate, steel faceplates, tie rods, and shear studs. The material models, element types, and boundary conditions used for the simulations are identical to those reported in Section 2. The shear studs and tie rods are spaced at 3 and 12 inches on center, respectively, along the height and length of the wall. The wall thickness is 12 inches. The compressive strength of the infill concrete is 7700 psi and the yield strength of the steel faceplates is 47 ksi. The bottom nodes of the baseplate are fixed.

The OOP loading was simulated by applying nodal forces to the steel and concrete elements at a given height above the base of the wall. Once the desired OOP load was reached, the load was held constant, and the wall was subjected to displacement-controlled cyclic IP loading at its top. The IP loading protocol consisted of seven load steps with two cycles per load step and a maximum drift of 1.6%.

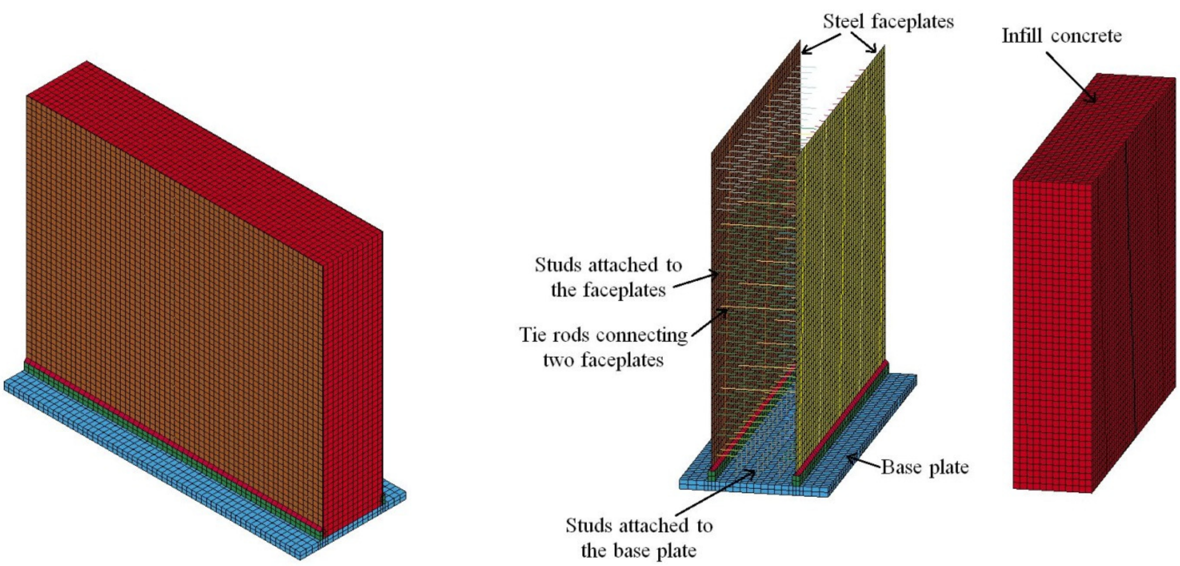

Fig. 7 – LS-DYNA model of CNSC1

The results of the parametric study are summarized in Table 3, where h_w is the height of the wall, l_w is the length of the wall, h_w / l_w is the aspect ratio, ρ_s is the reinforcement ratio, N is the axial load, $f_c^{'}$ is the concrete compressive strength, and A_c is the cross-sectional area of the infill concrete. Two values of a/d were considered for the OOP loadings: 1.5 and 3.0. For each value of a/d, multiple amplitudes of OOP shear stress were considered ($1\sqrt{f_c^{'}}$, $2\sqrt{f_c^{'}}$, and $3\sqrt{f_c^{'}}$); an OOP shear stress of $1\sqrt{f_c^{'}}$ had no material effect for simulation 2 and was not imposed for later numerical calculations. The effects of OOP loading on the IP response of piers with aspect ratios of 0.6 and 2, reinforcement ratios of 3.1 and 6.2%, and applied axial load of $0.2 f_c^{'} A_c$ were also investigated.

Table 3 - Summary of LS-DYNA simulations

Simulation	h_w / l_w	ρ_s (%)	N	a/d	OOP shear stress	IP capacity (kips)	% reduction in IP capacity
1	0.6	3.1	None	-	None	814	-
2	0.6	3.1	None	1.5	$1\sqrt{f_c^{'}}$	810	0
3	0.6	3.1	None	1.5	$2\sqrt{f_c^{'}}$	764	6
4	0.6	3.1	None	1.5	$3\sqrt{f_c^{'}}$	611	25
5	0.6	3.1	None	3	$1\sqrt{f_c^{'}}$	785	4
6	0.6	3.1	None	3	$2\sqrt{f_c^{'}}$	714	12
7	0.6	3.1	None	3	$3\sqrt{f_c^{'}}$	611	25
8	2	3.1	None	-	None	262	-
9	2	3.1	None	1.5	$2\sqrt{f_c^{'}}$	242	8
10	2	3.1	None	1.5	$3\sqrt{f_c^{'}}$	208	20
11	2	3.1	None	3	$2\sqrt{f_c^{'}}$	224	14
12	2	3.1	None	3	$3\sqrt{f_c^{'}}$	199	25
13	0.6	6.2	None	-	None	1400	-
14	0.6	6.2	None	1.5	$2\sqrt{f_c^{'}}$	1400	0
15	0.6	6.2	None	1.5	$3\sqrt{f_c^{'}}$	1370	2
16	0.6	6.2	None	3	$2\sqrt{f_c^{'}}$	1360	3
17	0.6	6.2	None	3	$3\sqrt{f_c^{'}}$	1270	9
18	0.6	3.1	$0.2 f_c^{'} A_c$	-	None	1270	-
19	0.6	3.1	$0.2 f_c^{'} A_c$	1.5	$2\sqrt{f_c^{'}}$	1240	2
20	0.6	3.1	$0.2 f_c^{'} A_c$	1.5	$3\sqrt{f_c^{'}}$	1170	8
21	0.6	3.1	$0.2 f_c^{'} A_c$	3	$2\sqrt{f_c^{'}}$	1160	9
22	0.6	3.1	$0.2 f_c^{'} A_c$	3	$3\sqrt{f_c^{'}}$	1050	17

Fig. 8a and Fig. 9a present the cyclic IP force-displacement relationships of SC walls subjected to OOP loadings of $1\sqrt{f_c^{'}}$, $2\sqrt{f_c^{'}}$, and $3\sqrt{f_c^{'}}$, for a/d equal to 1.5 and 3, respectively. The corresponding backbone curves for these simulations are presented in Fig. 8b and 9b, respectively, for a/d equal to 1.5 and 3. These walls have an aspect ratio of 0.6 and a reinforcement ratio of 3.1%. No axial load was applied. The peak IP lateral loads of these six SC walls are presented in Table 3: simulations 2 to 7. The peak IP capacity of the walls subjected to an OOP shear stress of $1\sqrt{f_c^{'}}$, $2\sqrt{f_c^{'}}$, and $3\sqrt{f_c^{'}}$ with a/d equal to 1.5 (3) is reduced by 0% (4%), 6% (12%), and 25% (25%), respectively, from the IP strength with no OOP load (=814 kips). The magnitude and location of the OOP load can have a significant effect on the IP capacity of SC walls. Importantly, an increase in a/d for a constant OOP load increases the (flexural) demand on the faceplates, which may affect IP behavior, both pre- and post-peak strength. Although, the OOP load effects the IP capacity, it does not appear to have a significant effect on initial stiffness, pinching, and rate of reloading/unloading of the SC walls, as observed in Fig. 8a and Fig. 9a.

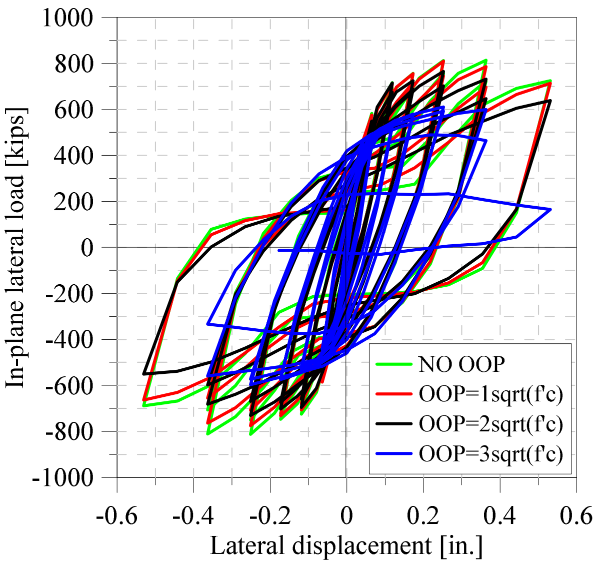

(a) force-displacement relationships

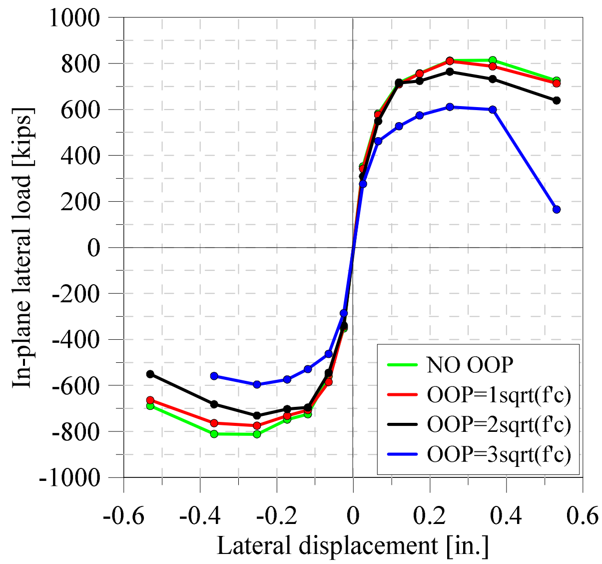

(b) backbone curves

Fig. 8 – IP behavior of SC walls, $h_w / l_w = 0.6$, $\rho_s = 3.1\%$, $N = 0$, $a/d = 1.5$

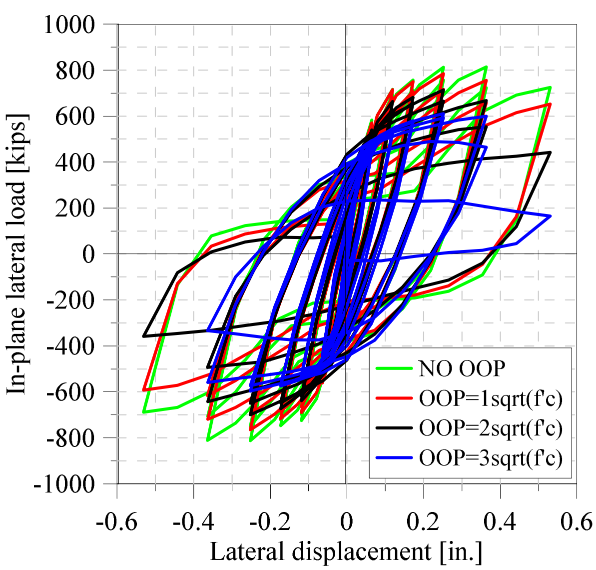

(a) force-displacement relationships

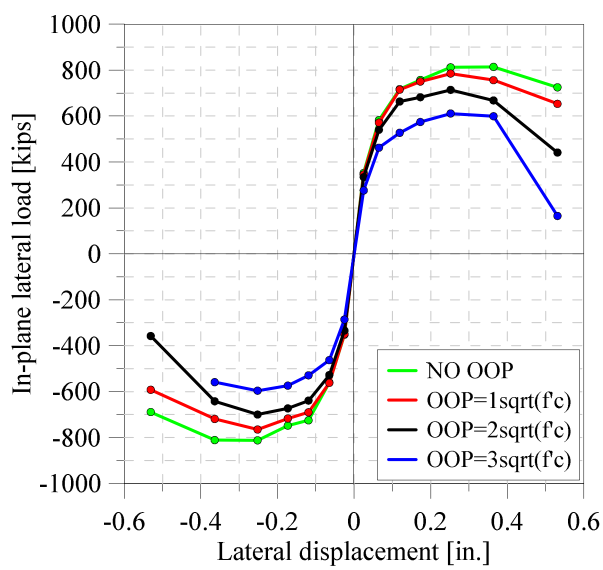

(b) backbone curves

Fig. 9 – IP behavior of SC walls, $h_w / l_w = 0.6$, $\rho_s = 3.1\%$, $N = 0$, $a/d = 3$

Simulations were performed on an SC wall with an aspect ratio of 2 to investigate the effect of a greater aspect ratio. No axial load was applied and the walls have a reinforcement ratio of 3.1%. Out-of-plane loadings of $2\sqrt{f_c^{'}}$ and $3\sqrt{f_c^{'}}$, and a/d of 1.5 and 3 were considered. Figure 10a presents the IP force-displacement relationships. The peak IP strengths are presented in Table 3: simulations 8 to 12. The OOP loading corresponding to a shear stress of $2\sqrt{f_c^{'}}$ and $3\sqrt{f_c^{'}}$, for $a/d = 1.5$ (3) reduce the peak IP strength by 8% (14%) and 20% (25%), respectively, from the IP strength with no OOP load (=262 kips). The cyclic backbone curves for each loading case are presented in Figure 10b. This outcome suggests the reduction in IP strength due to OOP loading is not significantly affected by aspect ratio: the reduction in IP strength for a shear-span to-wall thickness ratio of 3 and an OOP load corresponding to a shear stress of $3\sqrt{f_c^{'}}$ is approximately 25% for aspect ratios of 0.6 (simulation 7) and 2 (simulation 12).

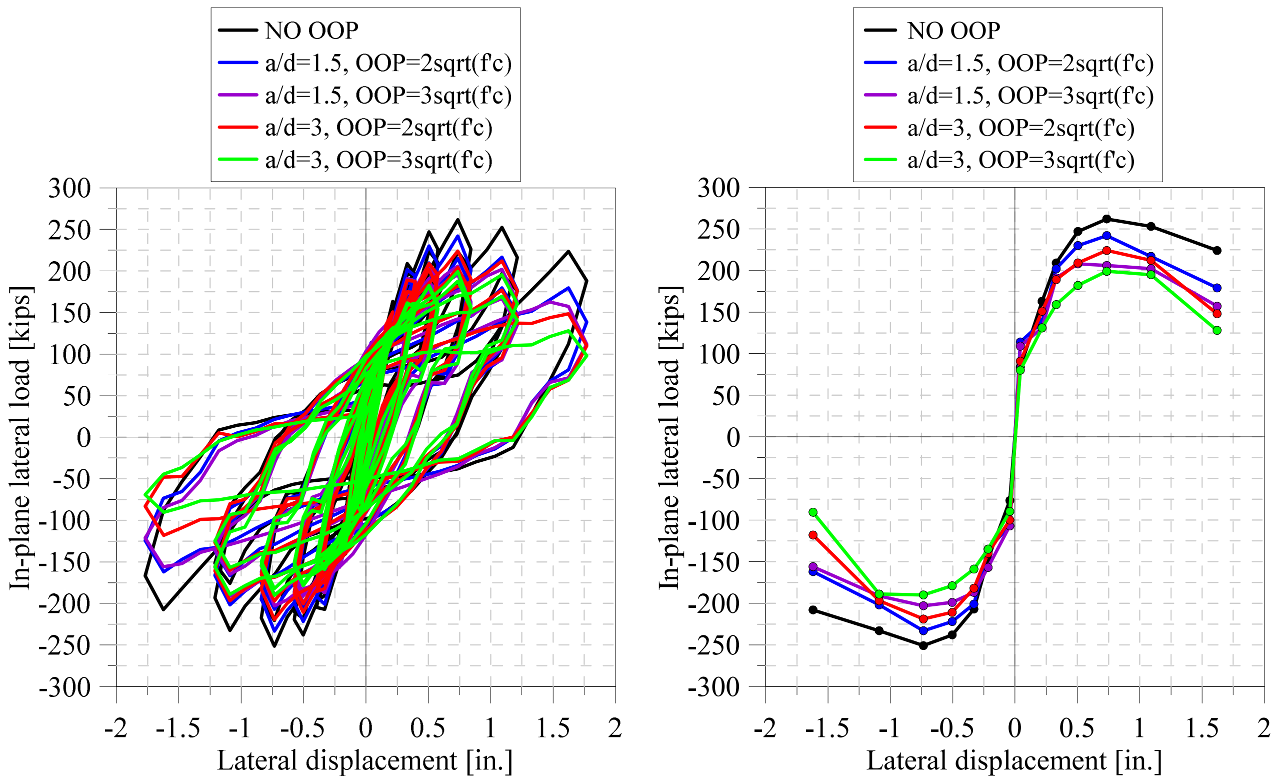

(a) force-displacement relationships (b) backbone curves

Fig. 10 – IP behavior of SC walls, $h_w / l_w = 2$, $\rho_s = 3.1\%$, $N = 0$

To investigate the effect of OOP loading on the IP lateral capacity of SC walls with large reinforcement ratios, the LS-DYNA models used for simulations 1, 3, 4, 6, and 7 were re-analyzed for a faceplate reinforcement ratio of 6.2%. The IP force-displacement relationships for OOP loadings corresponding to shear stresses of $2\sqrt{f_c^{'}}$ and $3\sqrt{f_c^{'}}$, and a/d of 1.5 and 3, and the corresponding backbone curves, are presented in Figures 11a and 11b, respectively. The peak IP strengths are presented in Table 3: simulations 13 to 17. A doubling of the reinforcement ratio increased the IP capacity, in the absence of OOP loading, by 72%. The IP capacity was reduced by 9% for a shear stress corresponding to an OOP load of $3\sqrt{f_c^{'}}$ and $a/d = 3$ with respect to the IP strength of the SC wall with no OOP load (=1400 kips), suggesting that OOP load may not have a significant effect on the IP response of the SC walls with high reinforcement ratios: an expected result, in the ranges of shear stress and a/d considered because the resultant axial stress demand (due to flexure) is relatively small.

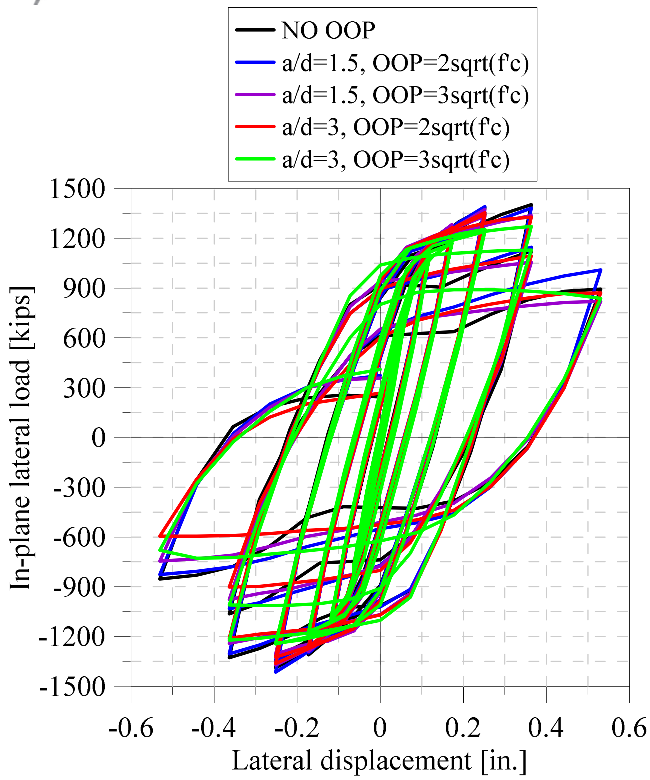

(a) force-displacement relationships

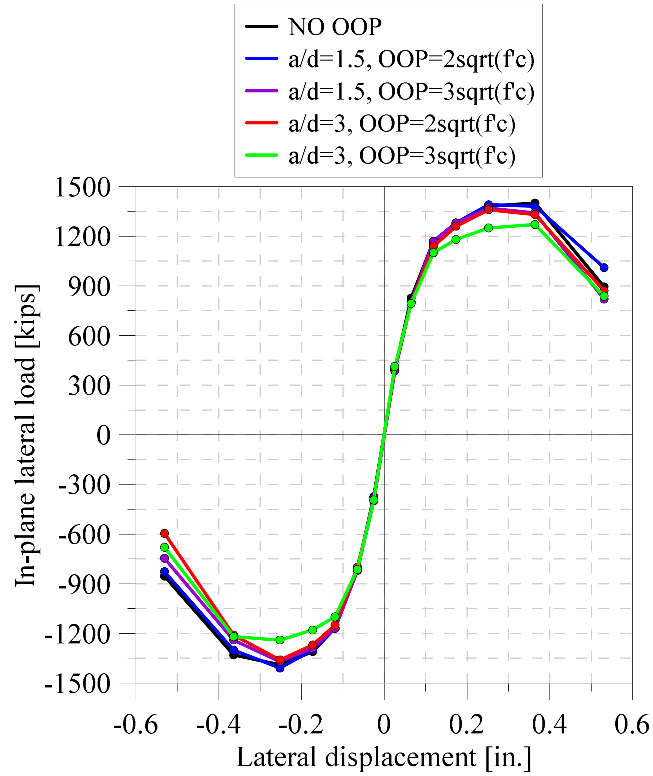

(b) backbone curves

Fig. 11 – IP behavior of SC walls, $h_w / l_w = 0.6$, $\rho_s = 6.2\%$, $N = 0$

To investigate the effect of axial compressive load on the response of SC walls, simulations 1, 3, 4, 6, and 7 were repeated with an applied axial compressive load equal to $0.2 f_c' A_c$. Fig. 12a and 12b present the cyclic IP force-displacement relationships and the cyclic backbone curves, respectively, of walls subjected to OOP loadings of $2\sqrt{f_c'}$ and $3\sqrt{f_c'}$, with a/d equal to 1.5 and 3. The IP lateral capacity of the SC wall (simulation 1) is increased by 60% when subjected to an axial compressive load of $0.2 f_c' A_c$. The peak IP strengths are presented in Table 3: simulations 18 to 22. The OOP loadings of $2\sqrt{f_c'}$ and $3\sqrt{f_c'}$ for a/d equal to 1.5 (3) reduce the peak IP strength of 1270 kips by 2% (9%) and 8% (17%), respectively. This axial compressive load reduced the effect of the OOP loading on the IP strength, which is an expected outcome. The reduction in IP strength due to OOP loading for the SC wall with $N = 0$ and $N = 0.2 f_c' A_c$, are 25% and 17%, respectively, for $a/d = 3$ and an OOP load corresponding to a shear stress of $3\sqrt{f_c'}$.

4. Summary and conclusions

A numerical model for simulation of the IP and OOP responses of SC wall piers was developed and validated using the test data of four large-scale rectangular SC walls subjected to in-plane cyclic loading and seven singly reinforced concrete beam specimens without shear reinforcement. The validated numerical model was used to investigate the effects of the OOP loading (i.e., magnitude and location) on the IP response of SC wall piers. The uniaxial compressive strength of the infill concrete (7700 psi) and the yield strength of the steel faceplates, both of which affect the IP and OOP response of SC walls, were not varied for the simulations reported here.

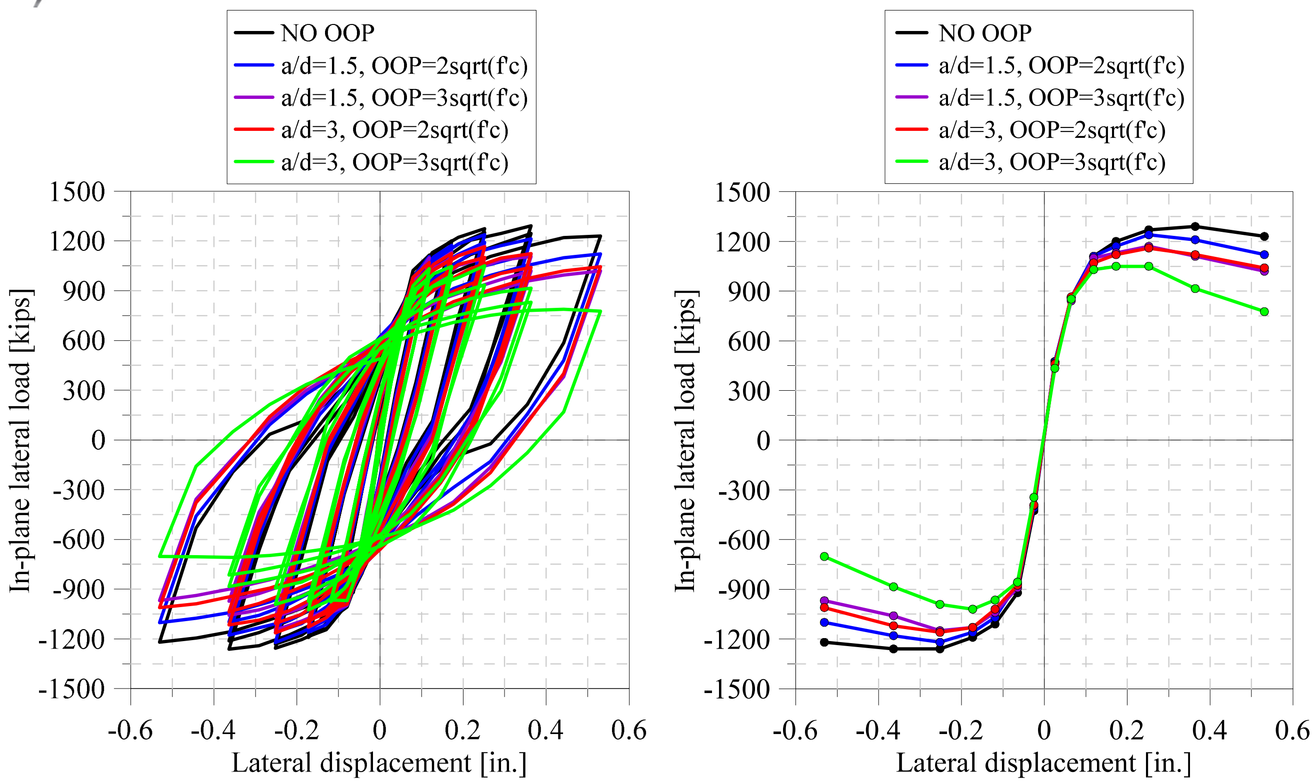

(a) force-displacement relationships (b) backbone curves

Fig. 12 – IP behavior of SC walls, $h_w / l_w = 0.6$, $\rho_s = 3.1\%$, $N = 0.2 f_c^{'} A_c$

Based on the simulations, OOP loading can have a significant effect on IP strength. Reductions in IP capacity due to OOP loading become more significant as the shear span-to-wall thickness and amplitude of the OOP load are increased.

Percentage reductions in IP strength are reported for ranges of aspect ratio, reinforcement ratio and axial compressive stress that might be expected in practice. These reductions are based on monotonic OOP and IP loadings. The percentage reductions are expected to increase for cyclic loadings, which is the subject of on-going investigation. The percentage reductions are also expected to vary as a function of concrete uniaxial compressive (and tensile) strength and steel faceplate yield strength, which is the subject of an on-going study.

5. References

[1] Yang Y, Jingbo L, Nie X, Fan J (2016): Experimental research on out-of-plane cyclic behavior of steel-plate composite walls. *Journal of Earthquake and Tsunami*, **10**, 1-16.

[2] Sener KC, Varma AH (2014): Steel-plate composite walls: experimental database and design for out-of-plane shear. *Journal of Constructional Steel Research*, **100**, 197-210.

[3] Sener KC, Varma AH, Ayhan D (2015): Steel-plate composite (SC) walls: out-of-plane flexural behavior, database, and design. *Journal of Constructional Steel Research*, **108**, 46-59.

[4] American Concrete Institute (ACI) (2006): Code requirements for safety-related concrete structures and commentary. *ACI349M-06*, Farmington Hills, USA.

[5] Bhardwaj SR, Kurt EG, Terranova B, Varma AH, Whittaker AS, Orbovic N (2015): Preliminary investigation of the effects of out-of-plane loading on the in-plane behavior of SC walls. *Proc., 21st Conference on Structural Mechanics in Reactor Technology SMiRT*, New Delhi, India.

[6] Kurt EG, Varma AH, Booth P, Whittaker AS (2013): SC wall piers and basemat connections: numerical investigation of behavior and design. *Proc., 22nd Conference on Structural Mechanics in Reactor Technology SMiRT*, San Francisco, USA.

[7] LS-DYNA (2012): Keyword User's Manual, Volume I. Version 971 R6.0.0, Livermore, USA.

[8] LS-DYNA (2012): Keyword User's Manual, Volume II. Version 971 R6.0.0, Livermore, USA.

[9] Epackachi S, Whittaker AS (2016): Experimental, numerical, and analytical studies on the seismic response of steel-plate concrete (SC) composite shear walls. *Technical report MCEER 16-0001*, University at Buffalo, State University of New York, Buffalo, USA.

[10] Epackachi S, Nguyen NH, Kurt EG, Whittaker AS, Varma AH (2013): In-plane seismic behavior of rectangular steel-plate composite wall piers. *Journal of Structural Engineering (ASCE)*, **141** (7), 1-9.

[11] Epackachi S, Whittaker AS, Varma AH, Kurt EG (2015): Finite element modeling of steel-plate concrete composite wall piers. *Engineering Structures*, **100**, 369-384.

[12] Epackachi S, Whittaker AS, Huang YN (2014): Analytical modeling of rectangular SC wall panels. *Journal of Constructional Steel Research*, **105**, 49-59.

[13] Epackachi S, Whittaker AS, Aref A (2016): Seismic analysis and design of steel-plate concrete wall piers. *Engineering Structures*, Under Review.

[14] Bresler B, Scordelis AC (1963): Shear strength of reinforced concrete beams. *ACI Journal Proceedings*, **60**, 51-74.

[15] Mphonde AG, Frantz GC (1985): Shear tests of high- and low-strength concrete beams without stirrups. *ACI Journal Proceedings*, **81**, 350-357.

[16] Wittmann FH, Rokugo K, Bruehwiler E, Mihashi H, Simonin P (1988): Fracture energy and strain softening of concrete as determined by means of compact tension specimens. *Materials and Structures*, **21** (121), 21-32.

[17] Comité Euro-International du Béton (CEB-FIP) (1993): *CEB-FIP model code 1990*. Thomas Telford, London.